BI-FRONTAL DEBRIS BED QUENCHING ANALYSIS USING COUNTER-CURRENT FLOW LIMITATION CONDITIONS

Kwang Won Lee* and Soon Heung Chang*

(Received May 16, 1988)

A generalized one-dimensional time-dependent quenching model is developed to assess the two-stage bi-frontal quenching process in cooling hot debris beds by top-flooding. The model is formulated by dividing the control mechanisms of the quenching process into the primary, namely counter-current flow limitation (CCFL) condition, and the secondary, i.e., the effects of subcooling of incoming coolant and steam cooling in dry channels on the quenching process. In order to evaluate the primary control mechanism, two methods are proposed by the name of Imaginary Tube Concept Approach (ITCA) and Packed Bed Concept Approach (PBCA). Comparison of each method with a few experimental data is presented. The predictions based on each method, specially that of ITCA, are in good agreement with the experimental data trends.

Key Words: One-Dimensional Time-Dependent Quenching Model, Bi-Frontal Debris Bed Quenching Process, Counter-Current Flow Limitation Condition, Coolant Subcooling Effect, Steam Cooling Effect

NOMENCLATURE

A : Bed total cross-sectional area
b : Wall thickness
C, C_p : Specific heat
D : Bed diameter
D_h : Bed hydraulic diameter
d : Particle diameter
G : Mass flux
g : Acceleration of gravity
H : Bed height
h : Enthalpy
$h_{l\nu}$: Latent heat of vaporization, $h_\nu - h_l$
$h'_{l\nu}$: Latent and sensible heat of vapor, $h'_\nu - h_l$
$h^*_{l\nu}$, $h^{**}_{l\nu}$: Modified parameters of $h_{l\nu}$ and $h'_{l\nu}$
j : Superficial velocity
j^* : Wallis dimensionless superficial velocity
L : Pool height
m : Mass
$\dot{m}$: Mass flow rate
q'' : Heat flux
T : Temperature
T_{po} : Initial particle temperature
T_{sat} : Saturation temperature
T_{li} : Initial pool temperature
T_l : Pool temperature
t : Time
Δt : Time interval
V_{front} : Modified quench front velocity
V : Control volume
z^* : Position of quench front

Greek Symbols

α : Void fraction
$\bar{\alpha}$: System mean void fraction
γ : Wall volume fraction for effective heat capacity of bed
ε : Porosity of packed bed
η : Bed permeability for turbulent flow
η_ν, η_l : Relative permeabilities of vapor and liquid for turbulent flow, rexpectively
κ : Bed permeability for laminar flow
κ_ν, κ_l : Relative permeabilities of vapor and liquid for laminar flow, respectively
λ_c : Capillary head
μ : Dynamic viscosity
ν : Kinematic viscosity
ρ : Density
σ : Surface tension
τ : Time duration for pool saturation

Subscripts

b : Bed above quench front
d : Downward progression
eff : Effective
f : Saturated liquid
i : Location of top of bed
l : Liquid
o : Location of quench front
p : Particle
u : Upward progression
v : Vapor
w : Wall

Superscripts

$\bar{}$: Time-averaged value
primed symbol($'$) : Superheated state in dry channel

1. INTRODUCTION

Water quenching of a hot debris bed, sensible heat removal of a superheated particles, is of interest in assessing the steam

*Department of Nuclear Engineering, Korea Advanced Institute of Science and Technology, Seoul 130-650, Korea.

spike phenomenon resulted from the interaction between core debris, water and coolability margins of a degraded light water reactor (LWR) core. The quenching phenomena are classified into two cases, i.e., top-flooding and bottom-flooding quenchings according to the direction of coolant flow path.

The bottom-flooding quenching, which is of special interest in assessing coolability margins of a degraded core, was satisfactorily modeled by Tung et al.(1985) and Ginsberg et al. (1983).

The top-flooding quenching is important in evaluating the steam spike phenomenon in containment and more complicate phenomenon than the bottom-flooding quenching. It has been experimentally and theoretically studied by Cho et al. (1982), Ginsberg et al.(1982a, 1982b), Gorham-Bergeron(1983) and Tung et al.(1985). The top-flooding quenching phenomenon was characterized experimentally as two-stage bi-frontal process and mainly controlled by counter-current flow limitation (CCFL) condition near the top of the bed. The two-stage bi-frontal process is composed of the downward frontal propagation and the upward frontal propagation stages. The downward frontal propagation leaves two regions: one is a fully quenched region in which particle temperature is equal to the saturation temperature and the other is a dry region in which particle temperature is nearly equal to the initial particle temperature.

Cho et al.(1982) suggested the quenching model based on flooding phenomena on imaginary tangled tubes in packed large particle bed. This model was able to estimate the bed heat flux and the quench front velocity for an one-stage quenching process, and the subcooling effect of coolant by introducing Ivey-Morris's vapor-liquid exchange model (Wallis and Block, 1978). The predictions show poor agreement with the experimental data except the case with highly subcooled coolant and hot particle bed. It seems to be caused by the one-dimensionality of the model.

Gorham-Bergeron(1983) proposed the analytic transient model based on the Lipinski bed dryout model. This model was able to predict the downward frontal propagation characteristics, namely, bed heat flux, quench front velocity, and constant finger fraction definded as the liquid volume fraction in the bed at any elevation. The steam superheating and the coolant subcooling effects on the quenching process were not considered in this model.

Cho et al.(1984) and Ginsberg(1985) reported that the steam generated at the quench front might be superheated by hot particles in the dry channels. Ginsberg(1985) suggested the model considering the effect of steam superheating. The model was based on the quasi-steady Lipinski bed dryout model, and modified to consider the effects of steam superheat on both the bed heat flux and the quench front propagation characteristics. The calculation results indicated that the effect of steam superheating is significant for the beds with small particles (<1 mm in diameter) and for the beds with high particle temperatures. Until now this model has been considered as the most general one. However the model is unsatisfactory to explain the phenomena because the model neglects the subcooling effect which has been reported to make dominant influence on the bed flux rate in the previous experimental studies (Cho et al., 1982, Ginsberg et al., 1982a, and Cho, Armstrong II & Chan, 1984), and cannot predict the volume fraction of the dry channels. In this model, the volume fraction of the dry channels (or the wetted channels) was based on the empirical constant rather than theoretical analysis.

The thermal inertial effect of the wall on the top-flooding quenching has been reported by Ginsberg et al.(1982a) and Tung et al.(1985). They found that liquid penetrates faster into the center region than the outer region of the bed if the wall is thick and heated up to the hot particle temperature. However, the liquid seepage was observed along the wall region with smaler thermal mass and larger porosity than those of the other region during the downward quenching process. Specially, Tung et al.(1985) showed that the liquid seepage and the nonuniformity of the bed make the prediction of the quenching process more difficult. They also claimed that the two-stage bi-frontal quenching process is not the general feature of the top flooding quenching but the special one of the quenching of the bed with uniform particles in highly heated thick wall. Therefore, in this paper, the two-stage bi-frontal quenching process is only considered that the special case able to be modeled mechanistically.

Through the survey on the previous models described above, it can be known that there is no available model to assess the top-flooding quenching satisfactorily. By this reason, the objective of this paper is to develop the generalized debris bed quenching model considering the effects of steam superheating, coolant subcooling and the thermal mass of the wall on the two-stage bi-frontal quenching process, mentioned above. To illustrate the necessity of the present

Table 1 Comparison of previous models with present model

Features \ Model	Quench process mode	Primary control mechanism	Steam cooling effect consideration	Subcooling effect consideration	Prediction capability for finger fraction
Ginsberg (1985)	two-stage	Lipinski dryout model	yes	no	no
Cho (1982)	one-stage	Flooding model	no	yes	no
Gorham (1985)	two-stage	Lipinski dryout model	no	no	yes
Present	two-stage	Lipinski dryout and flooding model	yes	yes	yes

study, the comparison of the previous models with the developed model is presented in Table 1. Consequently the developed model can predict all quenching parameters, i.e., bed heat flux, quench front velocity, finger fraction or volume fraction of quenched region, and steam cooled particle temperature etc.

2. ANALYSIS

2.1 Physical Model and Basic Assumptions

Based on the previous experimental observations, the top-flooding quenching is treated as the two-stage bi-frontal process.

During the initial downward frontal period the bed is assumed to consist of three regions. The first region, the partially quenched region above the quench front, consists of wetted (or quenched) channels and dry channels. The experiments by Cho, Armstrong II & Chan(1984) showed that wetted channels were joined together and formed as a single channel in the large particle bed (generally, above 1mm in diameter). However, Ginsberg et al.(1982a) claimed that the phenomenon didn't occur. The different observations seem to be caused by different measurement techniques and experimental conditions. It is considered in this paper that the agglomeration phenomenon of wetted channels may occur or not in the quenching process. In this model, the volume fraction of a single wetted channel or wetted multi-channels is evaluated by introducing the system mean void fraction concept (Wedekind and Beck, 1978), discussed later. For example, the volume fraction of the dry channels is obtained by multiplying the system mean void fraction by the total area of the bed. The second region, the quench front region, is composed of initial hot particles and incoming saturated liquid. The thickness of the quench front region is assumed to be shallow and negligible. At the quench front the supplied liquid is assumed to be completely vaporized and the bed is assumed to be partially quenched. The generated steam is supplied to dry channels above the quench front. The third region, the dry region below the quench front, is completely dry since coolant has not yet penetrated into the particles in this region.

During the upward frontal period, the residual stored energy is removed from the bed, therefore, the bed is completely quenched and filled with water.

The two-stage bi-frontal quenching process is shown schematically in Fig. 1. Here, for the convenience, wetted channels and dry channels are joined together, respectively.

To assess the quenching process, it is conveniently assumed that the process is divided into the primary and the secondary heat transfer process. the primary one is assumed to be controlled by CCFL condition. During this process, the basic quenching parameters, namely, bed heat flux, quench front velocity, and volume fraction of wetted channels can be calculated. The secondary one is considered to evaluate the effects of steam superheating and coolant subcooling on the basic quenching parameters.

The basic assumptions for the mathematical formulation of both heat transfer processes are listed below.

(1) The two-stage bi-frontal quenching process is regarded as a counter-current flow system, which is moving with the quench front velocity, with upward superheated steam and downward saturated water.

(2) The particle and coolant temperatures in the quenched and dry regions are same and both temperatures of each region are given as the volume-averaged values.

(3) The particle temperature in the quenched region cannot be restored. The mass and energy interactions between the wetted and the dry channels are neglected.

(4) All steam generated at the quench front region is superheated in the dry channels and condensed in the overlying pool if the pool is subcooled. If the pool is saturated, the steam penetrates the pool without condensation.

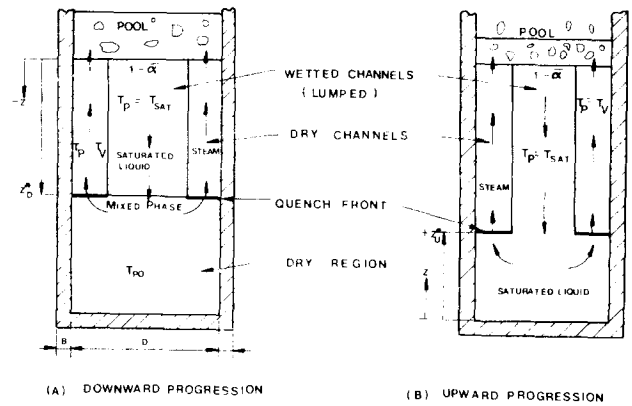

Fig. 1 Schematic diagram of physical model

Here, the assumption (2) is physically meaningful because heat transfer from the bed particulate to coolant (water or steam) is instantaneous for the millimeter particles generated by the non-explosive interactions of molten corium with water. The assumptions (3) and (4) are tentative and will be discussed at the following sections.

2.2 Model Description

(1) Primary Heat Transfer Process

(i) Mass Balance Equations

The time-dependent coolant mass balance equation is written as

$$\varepsilon\frac{\partial}{\partial t}[\rho_v\alpha+\rho_l(1-\alpha)]+\frac{\partial}{\partial z}(\rho_v j_v+\rho_l j_l)=0. \tag{1}$$

Integrating Eq.(1) over the specified control volume (See Fig. 1) with the concept of the system mean void fraction (Wedekind and Beck, 1978) and Leibnitz rule and assuming that the fluid densities of each phase are given as the volume-and time-averaged liquid density, ρ_l, and superheated vapor density, ρ_v', Eq.(1) becomes [See App. A]

$$\varepsilon(\rho_l-\rho_v')\,V_{front}=G_i-G_o \tag{2}$$

where

$$V_{front}=\begin{cases}(1-\bar{\alpha})\dfrac{dz_d^*}{dt} & \text{for downward progression (D.P.)}\\ -\bar{\alpha}\dfrac{dz_u^*}{dt} & \text{for upward progression (U.P.)}\end{cases} \tag{3}$$

and $\bar{\alpha}$ is the system mean void fraction, which is defined as

$$\bar{\alpha}=\frac{1}{z^*}\int_0^{z^*}\alpha(t,z)\,dz \tag{4}$$

The variable, z^*, in Eq.(4) is the position of the quench front

and given as

$$z^* = \begin{cases} z_d^* & \text{for D.P.} \\ z_u^* - H & \text{for U.P.} \end{cases} \tag{5}$$

At the quench front, since the complete vaporization occurs and all steam move into the dry channels, the total coolant mass flux at the quench front, G_o, is zero, i.e.,

$$-(\rho_l j_l)_o = (\rho_v j_v)_o \tag{6}$$

Then, the total mass balance equation is obtained as follows

$$\varepsilon(\rho_l - \rho'_v) V_{front} = G_{li} = \rho'_v j_{vi} + \rho_l j_{li} \tag{7}$$

where j_{li}, the liquid inlet superficial velocity, is considered to be negative because the liquid flows downward.

The mass balance equation on the liquid phase is

$$\varepsilon \frac{\partial}{\partial t}[\rho_l(1-\alpha)] + \frac{\partial}{\partial z}(\rho_l j_l) = -\Gamma_g \tag{8}$$

After manipulating as above, Eq. (8) becomes

$$\varepsilon \rho_l V_{front} = G_{li} - G_{lo} - \Gamma_g z^* \tag{9}$$

where Γ_g is the vapor generation rate in the wetted channels due to the decay heat source and the heat flux from the dry channels to the wetted channels. From basic assumption (3) and assuming that the decay heat source is negligible compared with the bed thermal inertia, the term of Γ_g in Eq. (9) is dropped. Then Eq. (9) becomes

$$G_{lo} = G_{li} - \varepsilon \rho_l V_{front} \tag{10}$$

(ii) Energy Balance Equation

The time-dependent energy balance equation for the coolant above the quench front is

$$\varepsilon \frac{\partial}{\partial t}[\rho_l h_l(1-\alpha) + \rho_v h_v \alpha] + \frac{\partial}{\partial z}[G_l h_l + G_v h_v] = -\nabla \cdot q''_b \tag{11}$$

Integrating Eq. (11) over the control volume by the same method as the derivation of Eq. (2) and combining with the mass balance equations (7) and (10), Eq. (11) becomes [See App. B]

$$q''_b = \rho'_v j_{vi}(h_{lv}^{**} - h_{lv}^*) - \varepsilon B \tag{12}$$

where

$$B = \begin{cases} [\rho'_v \bar{\alpha}(h_{lv}^{**} - h_{lv}^*) + h_v(\rho'_v - \rho_v)] \dfrac{dz_d^*}{dt} & \text{for D.P} \\ [\rho'_v \bar{\alpha}(h_{lv}^{**} - h_{lv}^*)] \dfrac{dz_u^*}{dt} & \text{for U.P} \end{cases} \tag{13}$$

and h_{lv}^* and h_{lv}^{**} are denoted as the modified latent heat of vaporization and the modified latent and sensible heat of vaporization for the cases existing liquid subcooling and vapor superheating, respectively. Those will be discussed in the section of subcooling effect. Eq. (12) indicates the bed heat flux removed by steam superheating. The energy balance equation for coolant on the quench front region is written as

$$q''_{front} = -G_{lo} h_{lv}^* \tag{14}$$

since the liquid reached the quench front is vaporized completely. The quench frontal propagation equation is derived as the following procedures.

The bed heat conduction equation is

$$\rho_p C_p(1-\varepsilon) \frac{\partial T_p}{\partial t} = -\nabla \cdot q'' \tag{15}$$

Taking volume-integral to Eq. (15) over the control volume with Leibnitz rule, Eq. (15) is transformed as

$$\rho_p C_p(1-\varepsilon)\left[\frac{d}{dt}\int_V T_p dV - \int_A T_p \frac{dz^*}{dt} dA\right] = -\int_A q'' dA \tag{16}$$

Introducing the system mean void fraction, $\bar{\alpha}$, as the volume fraction of the dry channels and integrating Eq. (16), it becomes

$$\rho_p C_p(1-\varepsilon)(T_{po} - T_{sat}) V_{front} = -q''_{front} \tag{17}$$

Substituting Eqs. (7), (10), and (14) into Eq. (17), the resulting equation, i.e., the quench frontal propagation equation, is

$$V_{front} = -\frac{\rho'_v j_{vi} h_{lv}^*}{\rho_p C_p(1-\varepsilon)(T_{po} - T_{sat}) + \varepsilon \rho'_v h_{lv}^*} \tag{18}$$

The total removal heat flux over control volume, q'', is obtained as

$$q'' = q''_{front} + q''_b \tag{19}$$

To find the quench front velocity, dz^*/dt, the vapor superficial velocity at top of the bed, j_{vi}, and the system mean void fraction, $\bar{\alpha}$, must be additionally determined.

The vapor superficial velocity can be obtained by combining the mass balance equation with the momentum balance equation. However, the system mean void fraction cannot be obtained by balance equations, therefore the constitutive equation for $\bar{\alpha}$ is needed. It will be discussed in the following sections.

(iii) Momentum Balance Equations

To determine the vapor superficial velocity at the top of the bed according to CCFL condition, two methods are suggested by the name of ITCA(Imaginary Tube Concept Approach) and PBCA(Packed Bed Concept Aproach). Here, ITCA is performed by considering the top-flooding quenching as the process controlled by counter-current flow limitation (CCFL) in a imaginary equivalent tube, which corresponds to the summation of tangled coolant paths in the bed. The CCFL condition is given as the well-known flooding correlations for packed beds. PBCA is accomplished by considering the quenching phenomenon as the process limited by a maximum bed permeability based on two-phase flow friction. The CCFL condition in this approach is quantified by introducing the Lipinski's separated flow formulation and a maximization technique.

For ITCA, the momentum equation of the system is replaced by the flooding correlation, which is given as

$$j_v^{*0.5} + j_l^{*0.5} = C \tag{20}$$

where

$$j_v^* = j_{vi}\sqrt{\frac{\rho'_v}{gD_h(\rho_l-\rho'_v)\varepsilon^2}} \tag{21a}$$

$$j_l^* = j_{li}\sqrt{\frac{\rho_l}{gD_h(\rho_l-\rho'_v)\varepsilon^2}} \tag{21b}$$

$$D_h = \frac{\varepsilon d}{6(1-\varepsilon)} \tag{21c}$$

$$C = \begin{cases} 0.775 \text{ in Wallis correlation} \\ \quad \text{(Ostensen and Lipinski, 1981)} \\ 0.875 \text{ in Marshall and Dhir correlation} \\ \quad \text{(Marshall and Dhir, 1983)} \end{cases} \tag{21d}$$

The vapor superficial velocity for ITCA is derived from Eq. (7) and Eqs. (20) and (21), then

$$j_{vi} = \frac{C^2 V_{ev}}{(1-DRS)^2}\left\{1-\left[DRS+\frac{|G_i|(1-DRS)}{C^2\rho_l V_{el}}\right]^{0.5}\right\}^2 \tag{22}$$

where

$$DRS = \left\{\frac{\rho'_v}{\rho_l}\right\}^{0.5} \tag{23a}$$

$$V_{ev} = \left\{gD_h(\rho_l-\rho'_v)\frac{\varepsilon^2}{\rho'_v}\right\}^{0.5} \tag{23b}$$

$$V_{el} = \left\{gD_h(\rho_l-\rho'_v)\frac{\varepsilon^2}{\rho'_l}\right\}^{0.5}. \tag{23c}$$

For PBCA, through combining Lipinski's separated flow momentum equations (Ginsberg, 1985 and Lipinski, 1984) with the mass balance equation, Eq. (7), the vapor superficial velocity is given as follows.

$$\frac{\rho'^2_v j^2_{vi}}{\eta}\left[\frac{1}{\rho_v\eta_v}+\frac{1}{\rho_l\eta_l}\right]+\frac{\rho_v j_{vi}}{\kappa}\left[\frac{\nu_v}{\kappa_v}-\frac{2|G_i|}{\rho_l\eta\eta_l}+\frac{\nu_l}{\kappa_l}\right]$$
$$+\frac{G_i^2}{\rho_l\eta\eta_l}-\frac{\nu_l|G_i|}{\kappa\kappa_l}-(\rho_l-\rho'_v)g\left[1+\frac{\lambda_c}{H}\right]=0 \tag{24}$$

where

$$\eta = \frac{\varepsilon^3 d}{1.75(1-\varepsilon)} \tag{25a}$$

$$\kappa = \frac{\varepsilon^3 d^2}{180(1-\varepsilon)^2} \tag{25b}$$

$$\eta_v = \alpha^5, \qquad \kappa_v = \alpha^3 \tag{25c}$$

$$\eta_l = (1-\alpha)^5, \qquad \kappa_l = (1-\alpha)^3. \tag{25d}$$

Here, κ, κ_v and κ_l indicate bed permeability, vapor and liquid relative permeabilities, respectively. Also η, η_v and η_l represent turbulent counterparts of κ, κ_v and κ_l. Bed permeability is similar to the inverse of a friction factor. Relative permeability quantifies an effective reduction in the permeability of the medium due to two-phase flow. The vapor superficial velocity corresponding to CCFL condition is given by maximizing Eq. (24) according to void fraction, α.

(iv) Constitutive Equation

The constitutive equation for the system mean void fraction, $\bar{\alpha}$, is given by the semiempirical correlation based on the drift flux model (Marshall and Dhir, 1983). It is written as

$$\bar{\alpha} = \left[2\left(1+\frac{j_{li}}{j_{vi}}\right)+3.44\frac{\sqrt{\frac{\sigma}{\rho_l d}}}{j_{vi}}\right]^{-1} \text{ for } \bar{\alpha}\le 0.3 \tag{26a}$$

$$\left[\sqrt{2}\left(1+\frac{j_{li}}{j_{vi}}\right)+5.24\frac{\sqrt{\frac{\sigma}{\rho_l d}}}{j_{vi}}\right]^{-1} \text{ for } \bar{\alpha}>0.3 \tag{26b}$$

In the primary heat transfer process, we can evaluate the basic quenching process parameters, i.e., the bed heat flux, q'', the quench front velocity, $\frac{dz^*}{dt}$, and the dry channels volume fraction, $\bar{\alpha}$, in Eqs. (14), (18), and (26).

(2) The Secondary Heat Transfer Process

(i) Steam Superheating Effect

Assume that steam enters the dry channels with the saturation temperature and leaves the region with the temperature equivalent to the particle temperature.

A lumped-parameter energy balance on the dry channels during the downward frontal period is given by Ginsberg(1985) as follows

$$m_p C_p\frac{dT_p}{dt} = \dot{m}_p C_p(T_{po}-T_p) - \dot{m}_v C_v(T_p-T_{sat}) \tag{27}$$

where

$$m_p = \bar{\alpha}(1-\varepsilon)\rho_p z_d^* A \tag{28a}$$

$$\dot{m}_p = \bar{\alpha}(1-\varepsilon)\rho_p\frac{dz_d^*}{dt}A \tag{28b}$$

$$\dot{m}_v = \rho_p C_p(1-\varepsilon)(1-\bar{\alpha})(T_{po}-T_{sat})\frac{dz_d^*}{dt}\frac{A}{h_{lv}^*} \tag{28c}$$

Similarly the energy balance for the upward frontal period is given as

$$m_p C_p\frac{dT_p}{dt} = -\dot{m}_v C_v(T_p-T_{sat}) \tag{29}$$

where

$$m_p = \bar{\alpha}(1-\varepsilon)\rho_p(z_u^*-H)A \tag{30a}$$

$$m_v = \rho_p C_p(1-\varepsilon)(1-\bar{\alpha})(T_p-T_{sat})\frac{dz_u^*}{dt}A \tag{30b}$$

After time interval, Δt, the steam temperature at the top of the bed is calculated by taking time-average on the solution of Eq. (27) [or Eq. (29)]. The time-averaged basic parameters obtained by the primary heat transfer process are recalculated at this temperature. The time-averaged bed heat flux removed by steam superheating is calculated from Eq. (12) by using the properties of vapor at this temperature.

(ii) Subcooling Effect of Incoming Coolant

For ITCA, Ivey-Morris' vapor-liquid exchange model (Wallis and Block, 1978) at the top of the bed is used for evaluating the inlet water subcooling effect. In this model, the latent heat of vaporization, h_{lv}, is modified as

$$h_{lv}^* = h_{lv}[1+\zeta(T_{sat}-T_l(t))] \tag{31}$$

where

$$\zeta = 0.1\left(\frac{\rho_l}{\rho_v}\right)^{0.75}\frac{C_{pl}}{h_{lv}}. \tag{32}$$

Since all steam are condensed in the overlying pool until the pool temperature is equal to saturation temperature, the

energy balance in the pool can be obtained as

$$m_l C_{pl}\frac{dT_l}{dt}=\rho'_v j_{vi} h^{**}_{lv} A - m_l C_{pl} T_l(t)\frac{dL}{dt}\frac{1}{L} \tag{33}$$

where

$$h'_{lv}=h'_v-h_f \tag{34}$$
$$h^{**}_{lv}=h'_{lv}[1+\zeta'(T_{sat}-T_l(t))] \tag{35}$$
$$\zeta=0.1\left(\frac{\rho_l}{\rho'_v}\right)^{0.75}\frac{C_{pl}}{h'_{lv}} \tag{36}$$
L=the pool height.

The second term on the right hand side of Eq. (33) is neglected by reason of having small value compared with other terms.

The time interval τ, for the saturation of the pool is derived from Eq. (33), then

$$\tau=m_l C_{pl}\ln[1+\zeta'(T_{sat}-T_{li})]\frac{1}{\rho'_v j_{vi} h^{**}_{lv}} \tag{37}$$

where m_l is the initial water mass supplied into the pool, and T_{li} is the initial temperature of water. Here, the water mass flowed in the bed and the penetrating steam mass is assumed to be negligible.

For PBCA, the parameters of ζ and ζ' in the above equation, are replaced by ;

$$\zeta=\frac{C_{pl}}{h_{lv}} \tag{38}$$
$$\zeta'=\frac{C_{pl}}{h'_{lv}} \tag{39}$$

The time-averaging latent heat of vaporization over the duration of quenching process Δt, is given by

$$\bar{h}^{*}_{lv}=h_{lv}\left\{\frac{\zeta(T_{sat}-T_{li})\tau}{\ln[1+\zeta(T_{sat}-T_{li})]}+(\Delta t-\tau)\right\}\frac{1}{\Delta t} \tag{40}$$

The time-averaged latent and sensible heat of vapor, $\bar{h}^{**}_{lv}$, is also given by replacing the terms, h_{lv} and ζ, by the terms, h'_{lv} and ζ' in Eq. (40).

The parameters, $\bar{h}^{*}_{lv}$ and $\bar{h}^{**}_{lv}$, are used for calculating the time-averaged basic parameters in the preceding sections.

(ii) Wall Thermal Inertia Effect

The wall effect of two-stage bi-frontal process is evaluated by adding the thermal mass of the wall to the bed thermal mass during the upward frontal progression. Thus the total thermal mass during the upward frontal progression is given as

$$(\rho_p C_p)_{eff}=(\rho_p C_p)_b+\gamma(\rho_p C_p)_w \tag{41}$$

where

b=*wall thickness*

$$\gamma=\frac{4b}{(1-\varepsilon)D} \tag{42}$$

3. CALCULATION PROCEDURES

The calculation procedures are schematically represented in Fig. 2. Here, it is noted that the computation is executed by two time steps, i.e., downward quenching period and upward quenching period, to be matched to the existing experimental data. During two quenching processes, the time-averaged steam temperature, $\bar{T}_v$ and modified parameters, $\bar{h}^{*}_{lv}$ and $\bar{h}^{**}_{lv}$ are used instead of T_v and h^{*}_{lv}, h^{**}_{lv}. The quench front velocities are also calculated as the time-averaged values, $V_d\left(=\frac{H}{\Delta t_d}\right)$ and $V_u\left(=\frac{H}{\Delta t_u}\right)$.

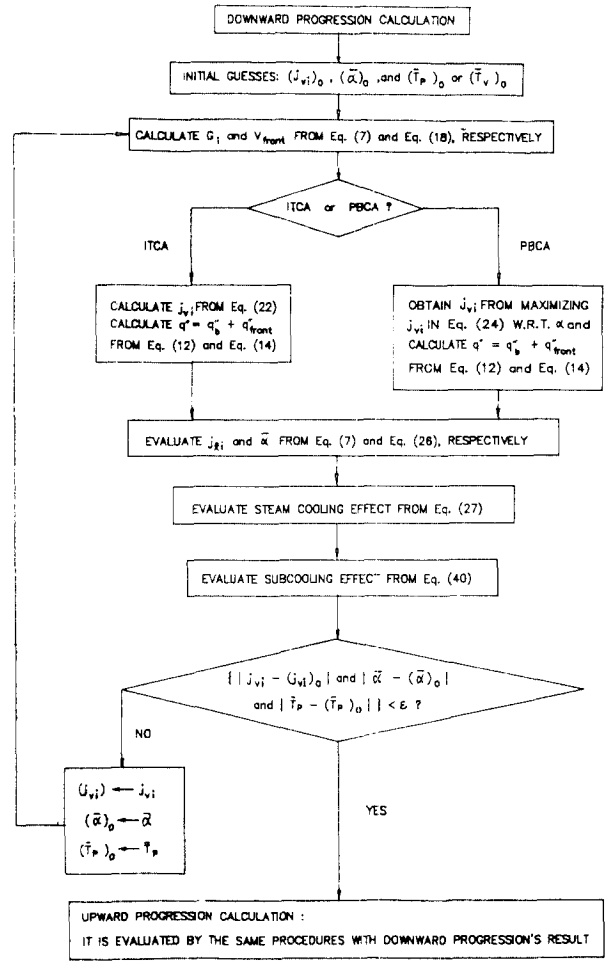

Fig. 2 Computational flow for the quenching process

4. RESULTS AND DISCUSSION

The prediction is performed for the selected experimental conditions and data (Ginsberg et al., 1982a and Cho, Armstrong II & Chan, 1984) listed in tables 2 and 3, respectively. It should be noted in the experimental data that the values about the bed heat flux of Ginsberg et al. experiments are averaged over the total quenching period without separating between the downward and upward bed heat fluxes.

In order to verify the validity of the present model, a comparison of the predictions of bed heat flux and quench front velocity with the experimental data is presented in Figs. 3a, 3b, 4a and 4b. Here, the calculation results for ITCA and PBCA are based on Marshall-Dhir flooding correlation in Eq. (21d) and Lipinski's latest relative permeabilities in Eqs. (25c & 25d), respectively. The comparison shows that the pre-

Table 2 Test conditions of previous experiments

Parameter	Range	
	Ginsberg et al.(1982a)	Cho et al.(1984)
packed bed particles	3mm spheres	3.1mm spheres
particle material	302 stainless	stainless steel, alumina
bed diameters	108.2mm	150mm
mass of particles	10-20kg	65kg for stainless steel, 28kg for alumina
mass of water	8-14kg	18.9kg
particle temperatures	260-700℃	500, 900℃
water temperatures	1-87℃	18-100℃
particle bed height	218-433mm	750mm
bed porosity	0.4	0.387
wall thickness	3.05mm	—

Table 3 Experiment data to be compared with the present model

Experiments number*	Bed** temperature (℃)	Water temperature (℃)	Downward quench front velocity (cm/sec)	Upward quench front velocity (cm/sec)	Area fraction of penetrating water column*** from bottom		Heat removal rate(kw/m²)	
					50	25	Downward	Upward
Cho. 1	500	100	0.23	0.08	0.19	0.20	836	873
Cho. 2	500	20	0.23	0.095	0.44	0.36	1431	785
Cho. 3	900	25	0.081	0.053	0.56	0.20	1069	829
Cho. 4	500	15	0.22	0.095	0.29	0.51	1527	699
Cho. 5	900	24	0.11	0.04	0.08	0.23	1236	802
Gin. 1	264	83	0.655	0.192	—	—	820#	
Gin. 2	265	89	0.709	0.197	—	—	780	
Gin. 3	262	23	0.764	0.264	—	—	990	
Gin. 4	545	88	0.192	0.098	—	—	900	
Gin. 5	261	1	0.846	0.372	—	—	1270	
Gin. 6	543	91	0.191	0.040	—	—	880	
Gin. 7	410	90	0.225	0.140	—	—	890	

Note
*Cho. 1 to 3 and Gin. 1 to 7 Stainless steel bed
Cho. 4 to 5 Alumina Bed
**Nominal initial bed temperature
***Nominal value
#These values are to be averaged over the total quenching period(Gin. 1 to 7)

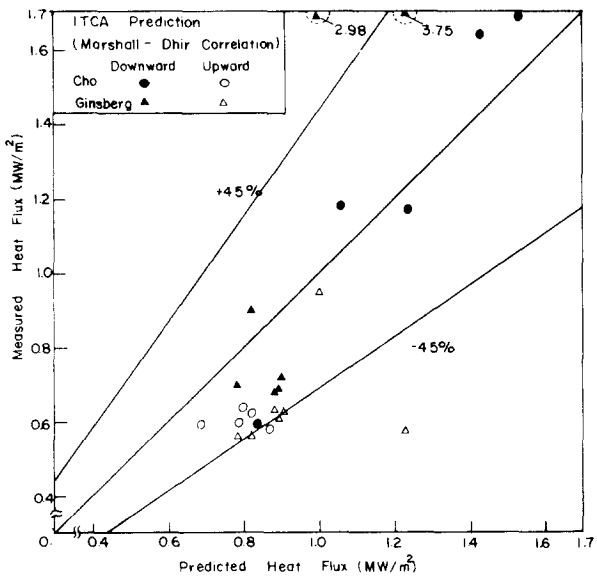

Fig. 3 (a) Comparison of bed heat fluxes predicted by ITCA with experimental data

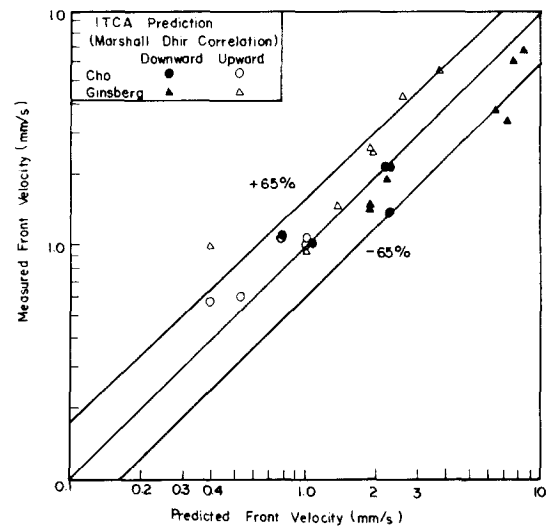

Fig. 3 (b) Comparison of quench front velocities predicted by ITCA with experimental data

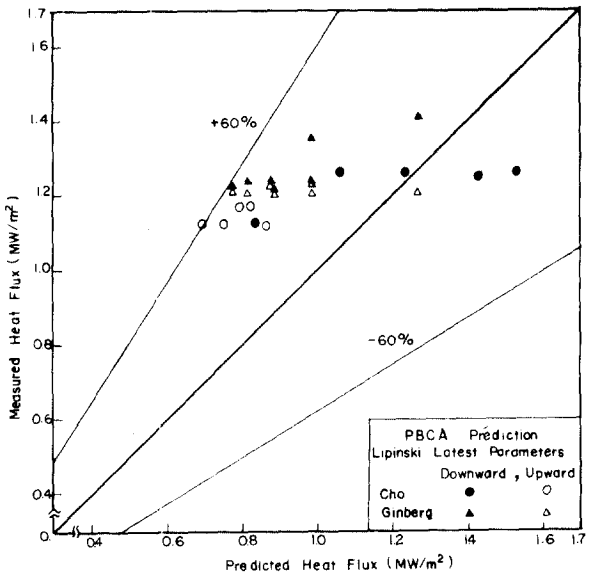

Fig. 4 (a) Comparison of bed heat fluxes predicted by PBCA with experimental data

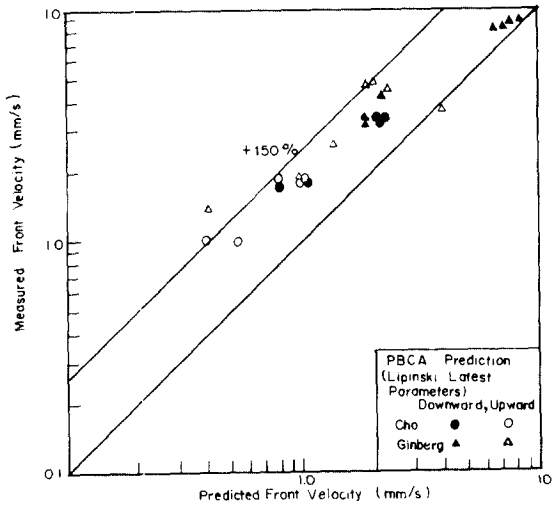

Fig. 4 (b) Comparison of quench front velocities predicted by PBCA with experimental data

dictions of ITCA and PBCA agree with the experimental data within error bounds of ±45% and ±60% for bed heat flux and ±65% and +150% for quench front velocity, respectively. This says that ITCA is superior to PBCA in the selected data range. The result is expected from the previous modeling experience (Tung et al., 1985, Ostensen & Lipinski, 1981, and Lipinski, 1984) that CCFL condition (flooding correlation) applied to ITCA is more promising than that of PBCA (Lipinski's methodology) in assessing the quenching or dryout phenomena of hot debris bed with large particle size (particle diameter ≥ 1mm). If the particle size is small, the above result may be reversed.

Specially, in Fig. 3a, the predictions of Ginsberg et al. data show large discrepancy. This discrepancy seems to be caused by the incompleteness of the data given by total averaged bed heat flux rather than the downward and upward bed heat flux.

Generally the predictions of ITCA are found to be underestimated while the predictions of PBCA are to be

Table 4 Four selected simulations for sensitivity analysis

Option run no.	Selected correlation or relative permeability	Steam cooling effect consideration	Subcooling effect consideration	Quench process mode
Run 1	Marshall-Dhir for ITCA Lipinski's latest for PBCA	yes	yes	Two-stage
Run 2	Wallis for ITCA Lipinski's linear for PBCA	yes	yes	Two-stage
Run 3	Same as run 1	no	yes	One-stage
Run 4	Same as run 1	yes	no	Two-stage

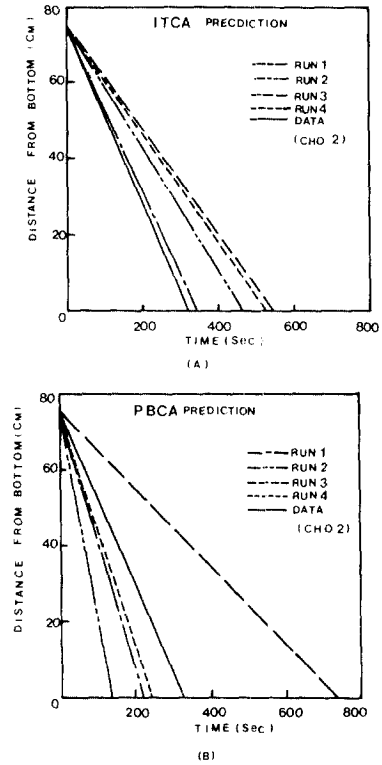

Fig. 5 Comparison of each predicted quench front velocity with experimental data of Cho 2

overestimated. It is also found that the cases with higher particle temperatures and relatively high subcooled water are better predictable than the cases with lower particle temperatures and saturated water. This trend seems to be related to the phenomenon of particle temperature recovery, which is observed experimentally but it is neglected in physical model.

To show the importance of the secondary heat transfer process and test the model sensitivity for the selection of CCFL parameters, C in Eq. (20) and relative permeabilities in Eq. (24), the four computer simulations are performed. The conditions of the four simulations are listed in Table 4.

The simulated results and their comparison with Cho, Armstrong II & Chan data are presented in Fig. 5. The comparison shows that the secondary heat transfer process is important and ITCA is superior to PBCA for modeling the

Table 5 Comparison of the predicted values of volume fraction of wetted channel and steam cooled particle temperature with Cho et al. experimental data

Experiment number	Comparison object	Area or volume fractions of wetted channel		Averaged steam cooled particle temperatures*	
Cho 1	Experimental data	0.19(z=50cm)	0.2(z=25cm)	426(z=50cm)	414(z=25cm)
	predicted values	**(a) 0.43		(a) 470.96	
		(b) 0.37		(b) 477.21	
Cho 2	Experimental data	0.44	0.36	512	448
	predicted values	(a) 0.44		(a) 440.30	
		(b) 0.37		(b) 478.37	
Cho 3	Experimental data	0.56	0.20	576	583
	predicted values	(a) 0.41		(a) 839.40	
		(b) 0.36		(b) 835.13	

Note:
*These values were measured when quench front reaches the bottom of the bed and averaged over the dry channel
**(a) Denotes the value computed by run 1 with ITCA
(b) Denotes the value computed by run 1 with PBCA

secondary heat transfer process. The reason is that the prediction based on ITCA is fairly improved by introducing the secondary heat transfer process while in PBCA prediction this improvement is not achieved. In PBCA prediction the steam cooling effect is dominant but the subcooling effect is negligible. This trend is contrary to the previous experimental observations. It also shows that both ITCA and PBCA are sensitive for selecting CCFL parameters.

The volume fraction of the wetted channels, $1-\bar{\alpha}$, and the steam cooled particle temperatures are compared with Cho, Armstrong II & Chan data in Table 5. The comparison shows that the predictions match roughly with the data. Here, it should be noted that the direct and reliable data to be compared with the predictions have not been reported yet. In fact the selected data in Table 5, specially for the steam cooled particle temperatures, were not based on the accurate experimental measurement but given by the indirect estimations reduced from the time responses of the thermocouples embedded in the bed during the quenching process. Therefore this comparison is not enough to assess the prediction capability of the model for the two parameters of the above. However it can be known from this comparison that the predictions are fairly encouraging even though the data are indirect and relatively rough.

5. CONCLUSION

The following conclusions can be drawn from the results of the preceding sections.

(1) The generalized one-dimensional time-dependent quenching model to evaluate the two-stage bi-frontal quenching process is developed.

(2) The secondary heat transfer process, namely, steam superheating and inlet coolant subcooling effects, is found to be important for evaluating the two-stage quenching process. Specially the subcooling effect in ITCA is found to be dominant for calculating the bed heat flux.

(3) All parameters of quenching process, i.e., bed heat flux, front velocity, volume fraction of dry channels, and steam cooled particle temperature are found to be roughly predicted.

(4) It is found that ITCA method is superior to PBCA method for the beds with a large particle diameter(d=3mm).

(5) The present model is applicable to evaluate two LWR safety issues, namely, steam spike phenomena in containment and concrete erosion with some modifications.

(6) The further studies to be recommended are as follows:
—The effect of mass and energy interactions between the wetted channels and the dry channels.
—The effect of steam penetration in the pool when the subcooling effect is modeled.
—The effect of the time delay of the quench front due to the internal heat resistance in more large particle beds.
—The scaling effect of container size for quenching process.
—The refinement of the flooding correlation, the constitutive equation for $\bar{\alpha}$, and the relative permeabilities.

REFERENCES

Cho, D.H., et al., 1982, "Debris Bed Quenching Studies", NUREG/CP-0027, Vol., 2, pp. 987~995.

Cho, D.H., Armstrong II, D.R. and Chan, S.H., 1984, "On the Pattern of Water Penetration into a Hot Particle Bed", Nucl. Tech., Vol. 65, pp. 23~31.

Ginsberg, T., et al., 1982a, "LWR Steam Spike Phenomenology: Debris Bed Quenching Experiments", NUREG/CP-2857, BNL-NUREG-51571.

Ginsberg, T., et al., 1982b, "Transient Core Debris Bed Heat Removal Experiments and Analysis", NUREG/CP-0027, Vol. 2, pp. 996~1009.

Ginsberg, T., et al., 1983, "Core Debris Quenching Heat Transfer Rates under Top-and Bottom-Reflood Conditions", Proceedings: International Meeting on LWR Severe Accident Evaluation, Vol. 2, Paper TS-18.7, Cambridge, MA, August 28~September 1.

Ginsberg, T., 1985, "Analysis of Influence of Steam Superheating on Packed Bed Quench Phenomena", AIChE Symposium Series: Heat Transfer-Denver 1985, Vol. 81, No. 245, pp. 273~281.

Gorham-Bergeron, E., 1983, "An Analytic Model for Predicting Dryout and Quench Behavior in a Volumetrically Heated Particle Bed", Proceedings: International Meeting on LWR Severe Accident Evaluation, Vol. 2, Paper TS-15.4, Cambridge, MA, August 28~September 1.

Lipinski, R.J., 1984, "A Coolability Model for Postaccident Nuclear Reactor Debris", Nucl. Tech., Vol. 65, pp. 53~66.

Marshall, J.S. and Dhir, V.K., 1983, "On the Counter-Current Flow Limitations in Porous Media", Proceedings: International Meeting on LWR Severe Accident Evaluation, Vol. 2, Paper TS-18.5, Cambridge, MA, August 28~Septem-

ber 1.

Ostensen, R.W. and Lipinski, R.J., 1981, "A Particle Bed Dryout Model Based on Flooding", Nucl. Sci. and Eng., Vol. 79, pp. 110~113.

Wallis, G.B. and Block, J.A., 1978, "Heat Transfer and Fluid Flows Limited by Flooding", AIChE Symposium Series: Heat Transfer-Research and Application, Vol. 74, No. 174., pp. 73~82.

Wedekind, G.L. and Beck, B.T., 1978, "A System Mean Void Fraction Model for Prediction Various Transient Phenomena Associated with Two-Phase Evaporating and Condensing Flows", Int. J. Multiphase Flow, Vol. 4, pp. 97~114.

Tung, V.X., Vu, H.X. and Dhir, V.K., 1985, "Quenching of Debris Bed Having Variable Permeability in the Axial and Radial Directions", Proceedings of Third International Topical Meeting on Reactor Thermal-Hydraulics, Vol. 2, Paper 19. G, Newport, Rhode Island, October 15~18.

APPENDIX

A. Derivation of Equation(2)

Integrating Eq. (1) over the control volume by using Leibnitz's rule, Eq. (1) becomes

$$\varepsilon\frac{d}{dt}\int_0^{z^*}[\rho_\nu\alpha+\rho_l(1-\alpha)]dz=[G(z,\ t)]_{z=0}-[G(z,\ t)]_{z=z^*}+\varepsilon[\rho_\nu\alpha+\rho_l(1-\alpha)]_{z=z^*}\frac{dz^*}{dt} \quad \text{(A. 1)}$$

Introducing the concept of system mean void fraction defined in Eq. (4), and assuming that the fluid densities are independent of position and given as the volume-averaged values for each region [see Fig. (1)], Eq. (A. 1) is rewritten as

$$\varepsilon\frac{d}{dt}\{[\rho'_\nu\bar{\alpha}+\rho_l(1-\bar{\alpha})]z^*\}=G_i-G_o+\varepsilon[\rho_\nu\alpha_o+\rho_l(1-\alpha_o)]\frac{dz^*}{dt} \quad \text{(A. 2)}$$

where the superscript prime denotes the state of superheated vapor and the subscripts i and o represent inlet and outlet, respectively.

Additionally, assuming that the fluid densities are only dependent of the particle temperatures in the occupying regions and independent of time during the given quenching period, and introducing the following approximations, i.e.,

$$\rho_l-\rho'_\nu\approx\rho_l-\rho_\nu \text{ and } \frac{d\bar{\alpha}}{dt}\approx 0 \text{ for a given quenching period} \quad \text{(A. 3)}$$

Eq. (A. 2) becomes

$$\varepsilon(\rho_l-\rho'_\nu)(\alpha_o-\bar{\alpha})\frac{dz^*}{dt}=G_i-G_o. \quad \text{(A. 4)}$$

Physically, the void fraction at the quench front, α_o, during downward progression is assumed to be 1 due to complete vaporization and during upward progression it is considered to be zero due to complete quenching.

Based on the above consideration, we obtain Eq. (2) from Eq. (A. 4).

B. Derivation of Equation(2)

In similar manner as App. A, integrating Eq. (11), yields

$$\varepsilon\frac{d}{dt}\{[\rho_l h_l(1-\bar{\alpha})+\rho_\nu h_\nu\bar{\alpha}]z^*\}=-q''_b+G_{li}h_l+G_{\nu i}h'_\nu-G_{lo}h_l-G_{\nu o}h_\nu+\varepsilon[\rho_l h_l(1-\alpha_o)+\rho_\nu h_\nu\alpha_o]\frac{dz^*}{dt} \quad \text{(B. 1)}$$

where

$$q''_b=\frac{1}{A}\int_A q''_b dA$$

$$\alpha_o=\begin{cases}1 \text{ for D.P.}\\ 0 \text{ for U.P.}\end{cases}$$

Using the properties of fluid takens by the averaged-values and the two-phase flow identities, Eq. (B. 1) becomes

$$\varepsilon[\rho_l h_l(\alpha_o-\bar{\alpha})+\rho'_\nu h'_\nu\bar{\alpha}-\rho_\nu h_\nu\alpha_o]\frac{dz^*}{dt}=-q''_b+(G_i-G_o)h_l+G_{\nu i}(h'_\nu-h_l)-G_{\nu o}(h_\nu-h_l). \quad \text{(B. 2)}$$

Substituting Eqs. (2), (6), (7), and (10) to Eq. (B. 2), yields

$$q''_b=G_{\nu i}(h'_\nu-h_\nu)-\varepsilon[\rho'_\nu\bar{\alpha}(h'_\nu-h_\nu)+h_\nu\alpha_o(\rho'_\nu-\rho_\nu)]\frac{dz^*}{dt}. \quad \text{(B. 3)}$$

To consider the coolant subcooling effect, in this model, $(h'_\nu-h_\nu)$ is replaced by $(h^{**}_{i\nu}-h^{*}_{i\nu})$. This fact is discussed at the section of (2) · (i) in 2. 2.

From Eq. (B. 3), we obtain Eq. (12) for downward and upward quench progress.